Int. J. Electrochem. Sci., 16 **(2021)** Article ID: 210661, doi: 10.20964/2021.06.63

International Journal of
ELECTROCHEMICAL
SCIENCE
www.electrochemsci.org

Short Communication

Synthesis and Intermediate-temperature Electrochemical Properties of Tm^{3+} and Gd^{3+} Double Doped Ceria-Chlorides Composite Electrolyte

Jilong Ma[*], *Yue Shen, Pan Yan, Lili Wang, Tingting Hu, Mengjuan Zhang, Yongjian Yang, Wenjian Wang, Guoquan Shao*[*]

College of Traditional Chinese Medicine, Bozhou University, Bozhou Anhui 236800, China
[*]E-mail: bzxymjl2019@163.com

Received: 3 March 2021 / *Accepted:* 20 April 2021 / *Published:* 30 April 2021

In this study, $Ce_{0.8}Gd_{0.1}Tm_{0.1}O_{2-\alpha}$ was synthesized by a nitrate-citric acid combustion method. $Ce_{0.8}Gd_{0.1}Tm_{0.1}O_{2-\alpha}$ powder and binary chlorides (NaCl, KCl) were mixed with the weight ratio kept at 3:1 to prepare $Ce_{0.8}Gd_{0.1}Tm_{0.1}O_{2-\alpha}$-(Na/K)Cl composite electrolyte. The crystal structures of $Ce_{0.8}Gd_{0.1}Tm_{0.1}O_{2-\alpha}$ and $Ce_{0.8}Gd_{0.1}Tm_{0.1}O_{2-\alpha}$-(Na/K)Cl were determined by X-ray diffraction (XRD). The AC impedance spectra of $Ce_{0.8}Gd_{0.1}Tm_{0.1}O_{2-\alpha}$-(Na/K)Cl were measured in the range of 450-700 °C and different oxygen partial pressures. The maximum conductivity and power density of the composite electrolyte reached 24.5 $mS \cdot cm^{-1}$ and 147.7 $mW \cdot cm^{-2}$ at 700 °C, respectively.

Keywords: Composite; Electrolyte; Fuel cell; Oxygen partial pressure; Conductivity

1. INTRODUCTION

Solid electrolytes are widely used in the field of solid oxide fuel cells (SOFCs), the chemical industry, metallurgy and in sensors due to their excellent ionic conductivities [1–5]. Traditional SOFCs used yttrium oxide stabilized zirconia (YSZ) as electrolyte and the working temperature was generally higher than 800 °C which led to high cost and limited the practical application [6–12]. The doped CeO_2-based solid electrolyte had higher ionic conductivity and lower activation energy than YSZ, which was a good oxygen ion conductor [13-16]. For example, Arabaci et al. synthesized Sm^{3+} doped CeO_2 using a Pechini method [14]. Reports showed that the doping effect of rare earth oxides is better than those of alkaline earth oxides, and Sm^{3+} and Gd^{3+} are the best [17-21]. In general, if the radius of the doped ion is close to that of the main cation in the lattice, it will cause the smallest expansion or contraction. It can reduce the binding enthalpy between the doped cation and oxygen vacancy, improve the ion mobility and achieve higher conductivity. The radius of Tm^{3+} ion is 0.088 nm, which is close to that of Ce^{4+}

(0.087 nm). In addition, most CeO_2-based solid electrolyte materials are prepared by the liquid phase method. This is because compared with the traditional solid-state synthesis, the liquid phase method can produce high-purity uniform nano powder and has a lower reaction temperature. Therefore, $Ce_{0.8}Gd_{0.1}Tm_{0.1}O_{2-\alpha}$ was synthesized by a nitrate-citric acid combustion method in this study [22-25].

The main method to improve the conductivity of solid electrolytes is to construct composite electrolyte. In recent years, ceria-carbonates, ceria-chlorides and ceria-sulfates composite electrolytes have shown theirs advantages in solid electrolyte research [26-29]. Therefore, $Ce_{0.8}Gd_{0.1}Tm_{0.1}O_{2-\alpha}$-(Na/K)Cl was prepared by mixing binary chlorides with $Ce_{0.8}Gd_{0.1}Tm_{0.1}O_{2-\alpha}$ powder in this study. The crystal structures of $Ce_{0.8}Gd_{0.1}Tm_{0.1}O_{2-\alpha}$ and $Ce_{0.8}Gd_{0.1}Tm_{0.1}O_{2-\alpha}$-(Na/K)Cl were determined by X-ray diffraction (XRD). The electrical properties of $Ce_{0.8}Gd_{0.1}Tm_{0.1}O_{2-\alpha}$-(Na/K)Cl composite electrolyte were measured by AC impedance technique in the range of 450-700 °C.

2. EXPERIMENTAL

$Ce_{0.8}Gd_{0.1}Tm_{0.1}O_{2-\alpha}$ was synthesized by a nitrate-citric acid combustion method. According to the required molar ratio, $(NH_4)_2Ce(NO_3)_6$ was dissolved in water and Tm_2O_3 and Gd_2O_3 were dissolved in nitric acid. The mixed solution of Tm^{3+}, Ce^{4+} and Gd^{3+} was prepared. Citric acid with a molar ratio of 2 to metal ions was added, and the *p*H value of the mixed solution was adjusted to 7 with NH_4OH. At 80 °C, the sol was evaporated to remove most of the water, and then heated to spontaneous combustion to obtain the primary powder. Finally, $Ce_{0.8}Gd_{0.1}Tm_{0.1}O_{2-\alpha}$ powder was obtained by calcination at 900 °C for 5 h. $Ce_{0.8}Gd_{0.1}Tm_{0.1}O_{2-\alpha}$ powder and binary chlorides (NaCl, KCl) were mixed thoroughly with the weight ratio kept at 3:1. $Ce_{0.8}Gd_{0.1}Tm_{0.1}O_{2-\alpha}$-(Na/K)Cl was prepared by it pressing into a disc in the mold and then heating at 750 °C for 1 h.

The gel was heated from room temperature to 900 °C using a thermogravimetry analysis and differential scanning calorimetry (TGA-DSC) method. The crystal structures of $Ce_{0.8}Gd_{0.1}Tm_{0.1}O_{2-\alpha}$ and $Ce_{0.8}Gd_{0.1}Tm_{0.1}O_{2-\alpha}$-(Na/K)Cl were determined by X-ray diffraction (XRD). The morphology of $Ce_{0.8}Gd_{0.1}Tm_{0.1}O_{2-\alpha}$-(Na/K)Cl was observed by scanning electron microscopy (SEM). The AC impedance spectra of $Ce_{0.8}Gd_{0.1}Tm_{0.1}O_{2-\alpha}$-(Na/K)Cl were measured in the range of 450-700 °C and different oxygen partial pressures with CHI660E electrochemical workstation. The H_2/O_2 fuel cell was assembled and its performance was studied.

3. RESULTS AND DISCUSSION

In order to understand the decomposition of $Ce_{0.8}Gd_{0.1}Tm_{0.1}O_{2-\alpha}$ gel and the formation of crystalline phase, the TGA-DSC analysis was carried out, as shown in Fig. 1. From Fig. 1, the 15% weight loss below 100 °C corresponds to the evaporation of water in the gel. 12 % weight loss between 150 °C and 260 °C is the decomposition of nitrate and ammonium salt, corresponding to a broad endothermic peak on the DSC curve [18-19]. It was observed that the gel rapidly expanded and a large amount of yellow smoke was generated in the experiment. The 66 % weight loss between 260 °C and

265 °C corresponds to the strong exothermic peak of 263 °C on DSC curve. In this process, citric acid self-combustion reaction occurs and a lot of heat is released. After 320 °C, the weight loss almost disappears, and it can be inferred that the decomposition has been basically completed [21]. After 580 °C, the quality of the gel does not change completely, indicating the formation of fluorite phase. Therefore, $Ce_{0.8}Gd_{0.1}Tm_{0.1}O_{2-\alpha}$ is calcined at 900 °C for 5 h.

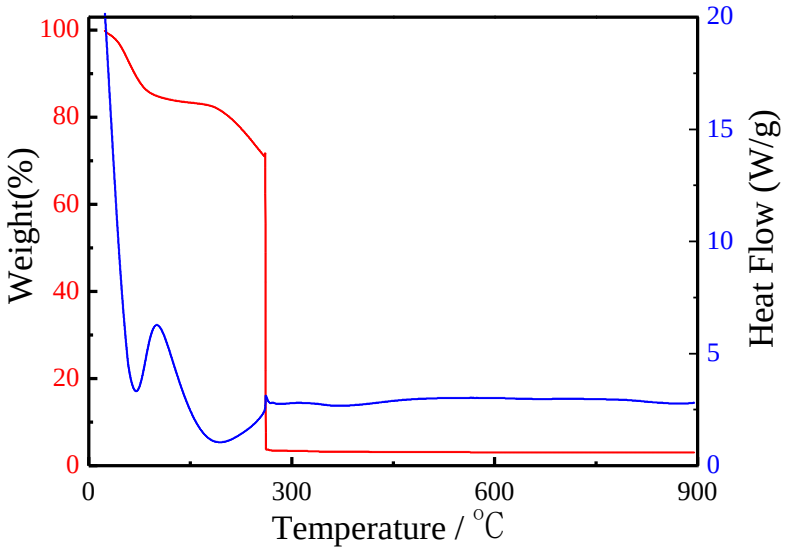

Figure 1. TGA-DSC curve of gel ($Ce_{0.8}Gd_{0.1}Tm_{0.1}O_{2-\alpha}$) from room temperature to 900 °C.

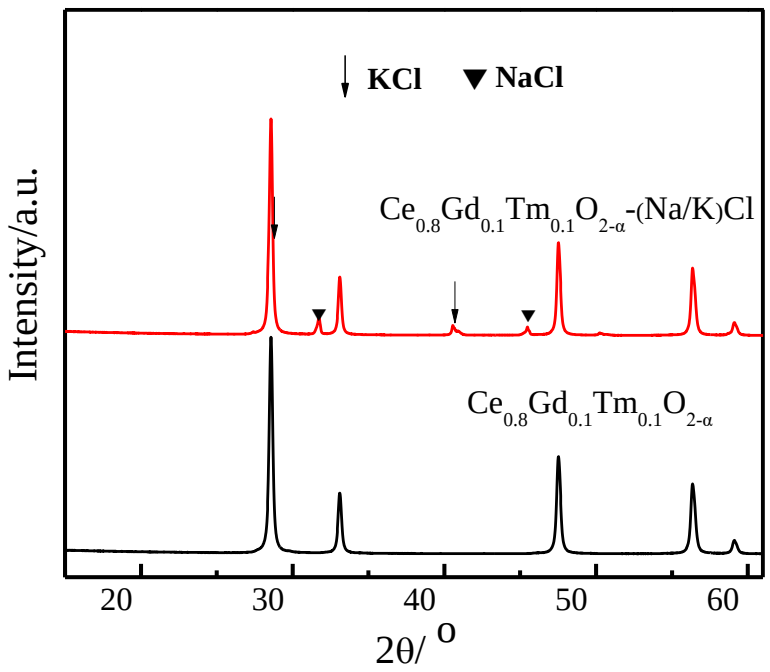

Figure 2. XRD spectra of $Ce_{0.8}Gd_{0.1}Tm_{0.1}O_{2-\alpha}$ and $Ce_{0.8}Gd_{0.1}Tm_{0.1}O_{2-\alpha}$-(Na/K)Cl after calcined at 900 °C for 5 h.

Fig. 2 is the XRD spectra of combustion products after being calcined at 900 °C for 5 h. It can be seen that all the diffraction peaks of $Ce_{0.8}Gd_{0.1}Tm_{0.1}O_{2-\alpha}$ are consistent with the standard spectrum (JCPDS, 00-046-0507) and there are no other peaks. It shows that Tm^{3+} and Gd^{3+} replace part of Ce^{4+} in the lattice, forming CeO_2 solid solution [17-18]. Therefore, it can be considered that the $Ce_{0.8}Gd_{0.1}Tm_{0.1}O_{2-\alpha}$ powder with a cubic fluorite structure was directly synthesized by nitrate-citric acid combustion method [21-23]. In Fig. 2, we can see that in addition to the diffraction peaks of $Ce_{0.8}Gd_{0.1}Tm_{0.1}O_{2-\alpha}$, there are also weak peaks of NaCl and KCl in the composite electrolyte. This may be because the chlorides are molten during heat treatment. When the composite electrolyte powder cools from 900 °C to room temperature, the molten binary chlorides cannot crystallize, and most of them exist in amorphous state. Therefore, there are only weak NaCl and KCl peaks in the XRD spectrum of the composite electrolyte.

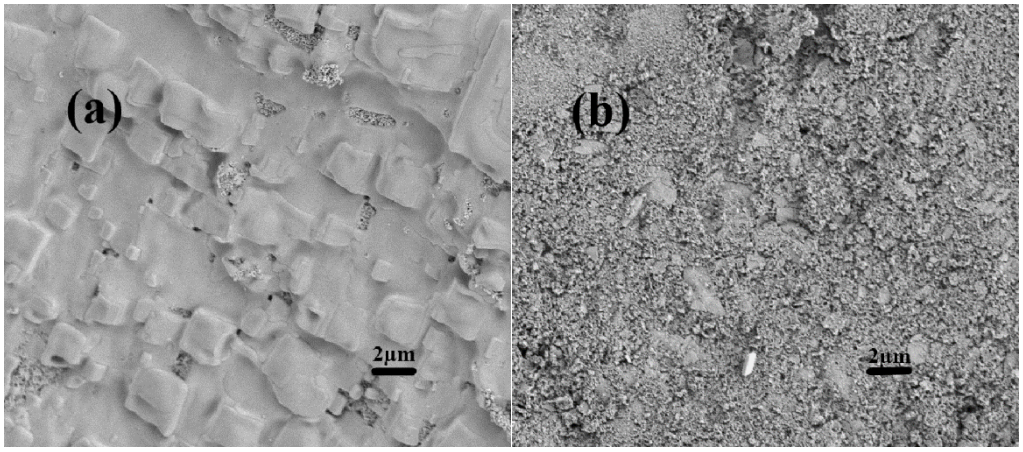

Figure 3. SEM images (a) external, (b) cross-sectional of $Ce_{0.8}Gd_{0.1}Tm_{0.1}O_{2-\alpha}$-(Na/K)Cl after heat treatment at 750 °C.

Fig. 3 shows the external and cross-sectional SEM images of the composite electrolyte. It can be seen from the picture that the composite electrolyte disc obtained after heat treatment at 750 °C for 1 h has no holes. The cross-sectional SEM image shows that $Ce_{0.8}Gd_{0.1}Tm_{0.1}O_{2-\alpha}$ and (Na/K)Cl are interconnected in three dimensions and closely combined [26-28]. The molten chlorides completely covered the $Ce_{0.8}Gd_{0.1}Tm_{0.1}O_{2-\alpha}$ powder to form a uniform composite.

Fig. 4 shows the relationship between the conductivities and temperatures in the range of 450-700 °C of $Ce_{0.8}Gd_{0.1}Tm_{0.1}O_{2-\alpha}$-(Na/K)Cl and others reported in the literature [30-32]. The conductivities of $Ce_{0.8}Gd_{0.1}Tm_{0.1}O_{2-\alpha}$-(Na/K)Cl increased with the increase of temperatures. The maximum conductivity of the composite electrolyte reached 24.5 $mS \cdot cm^{-1}$ at 700 °C. The conductivities are close to that of $Ce_{0.8}Sm_{0.2}O_{2-\alpha}$-5%$Al_2O_3$ [30] composite electrolyte and higher than those of single $Ce_{0.8}Zr_{0.2}O_{1.9}$ [32] and composite $Ce_{0.8}Gd_{0.1}Sm_{0.1}O_{2-\alpha}$-$Na_2CO_3$ [31] electrolytes at the same temperatures. The results show that the chlorides eutectic and $Ce_{0.8}Gd_{0.1}Tm_{0.1}O_{2-\alpha}$ compound form a "highway" transmission channel in the interface region between the two components, which greatly reduces the migration activation energy which must be overcome in conducting ion migration.

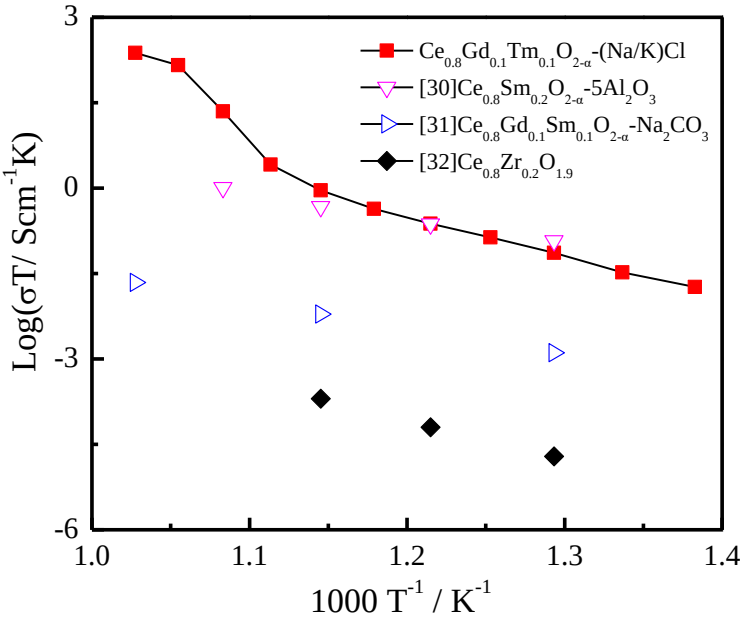

Figure 4. The relationship between the conductivities and temperatures in the range of 450-700 °C.

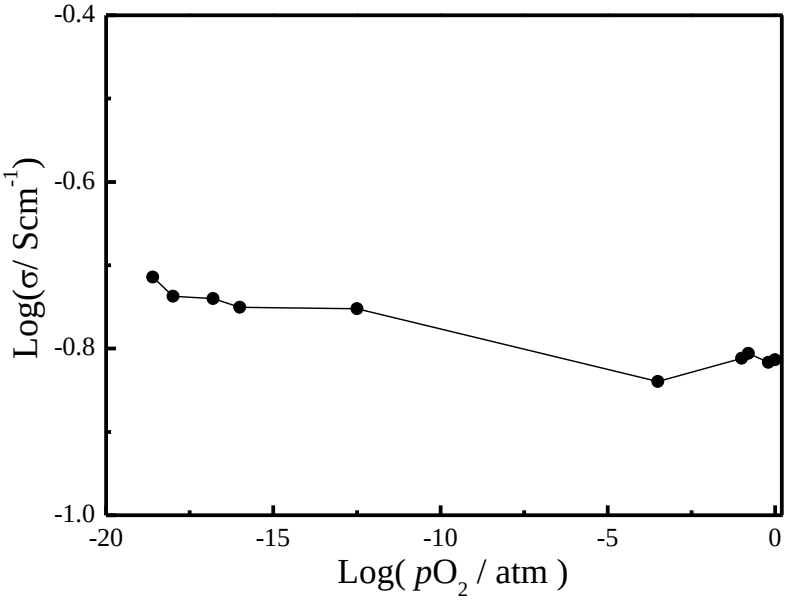

Figure 5. The relationship between the conductivities and different oxygen partial pressures of $Ce_{0.8}Gd_{0.1}Tm_{0.1}O_{2-\alpha}$-(Na/K)Cl.

The relationship between the conductivities and different oxygen partial pressures of $Ce_{0.8}Gd_{0.1}Tm_{0.1}O_{2-\alpha}$-(Na/K)Cl at 700 °C is shown in Fig. 5. For the relationship between oxygen partial pressures and conductivities, when log $\sigma \sim$ log (pO_2) is a horizontal straight line, it shows that the electrolyte has ionic conductivity. Otherwise, the electrolyte has electron (or hole) conductivity in addition to ionic conductivity. It can be seen from Fig. 5 that the conductivities of $Ce_{0.8}Gd_{0.1}Tm_{0.1}O_{2-\alpha}$-(Na/K)Cl almost do not change with oxygen partial pressures in the range of $pO_2 = 10^{-4} \sim 1$ atm, indicating that the composite electrolyte is a good oxygen ion conductor [33]. In the range of $pO_2 = 10^{-}$

^{19}～10^{-12} atm, the conductivities increase slightly with the decrease of oxygen partial pressures, which indicates that there is a small amount of electron conduction besides oxygen ion conduction. Taub et al. found that the electron conductivity of $Ce_{0.8}Gd_{0.1}Co_{0.02}O_{2-\alpha}$ was proportional to $pO_2^{-1/6}$ in a reductive atmosphere [34]. This result is in agreement with the previous findings that the composite electrolyte is a good oxygen ion conductor in an oxidizing atmosphere [33, 35], however, it is different from Taub's report [34]. This shows that the composite electrolyte can inhibit the electronic conductivity.

The H_2/O_2 fuel cell using $Ce_{0.8}Gd_{0.1}Tm_{0.1}O_{2-\alpha}$-(Na/K)Cl as electrolyte was assembled and its performance was studied with oxygen and hydrogen as oxidant and fuel gas, respectively. The current density increased with the decrease of discharge voltage, as shown in Fig. 6. The maximum power density of $Ce_{0.8}Gd_{0.1}Tm_{0.1}O_{2-\alpha}$-(Na/K)Cl reached 147.7 mW·cm^{-2} and corresponding current density was 295.4 mA·cm^{-2} at 700 °C, which is higher than that of $Ce_{0.8}Er_{0.1}Gd_{0.1}O_{2-\alpha}$-$K_2SO_4$-$Li_2SO_4$ (98.1 mW·cm^{-2}) at 700 °C [36]. This shows that the design of $Ce_{0.8}Gd_{0.1}Tm_{0.1}O_{2-\alpha}$-(Na/K)Cl composite electrolyte is reasonable, which is more conducive to the improvement of electrical properties at medium temperature.

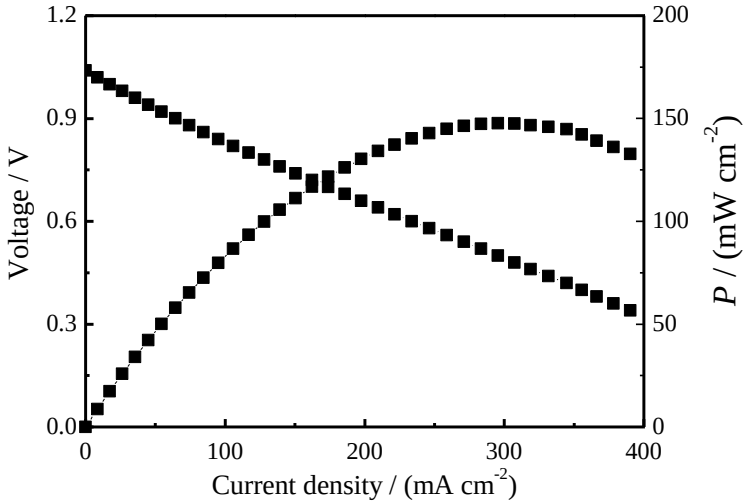

Figure 6. The H_2/O_2 fuel cell using $Ce_{0.8}Gd_{0.1}Tm_{0.1}O_{2-\alpha}$-(Na/K)Cl as electrolyte at 700 °C.

4. CONCLUSIONS

In this study, Tm^{3+} and Gd^{3+} co-doped CeO_2 powder was mixed with NaCl and KCl to prepare $Ce_{0.8}Gd_{0.1}Tm_{0.1}O_{2-\alpha}$-(Na/K)Cl composite electrolyte. The cross-sectional SEM image showed that $Ce_{0.8}Gd_{0.1}Tm_{0.1}O_{2-\alpha}$ and (Na/K)Cl were interconnected uniformly in three dimensions and closely combined. The maximum conductivity and power density of the composite electrolyte reached 24.5 mS·cm^{-1} and 147.7 mW·cm^{-2} at 700 °C, respectively. The log σ ～ log (pO_2) result indicated that $Ce_{0.8}Gd_{0.1}Tm_{0.1}O_{2-\alpha}$- (Na/K)Cl was a good oxygen ion conductor in the range of $pO_2 = 10^{-4}$～1 atm.

ACKNOWLEDGEMENTS
This work was supported by the Natural Science Project of Anhui Province (No. KJ2017A709, KJ2019A1304), Anhui Provincial Key Laboratory of traditional Chinese medicine raw material research and development (No. KLAHE18032).

CONFLICTS OF INTEREST
The authors declare no conflicts of interest.

References

1. L. Bi, S.P. Shafi, E.H. Da'as and E. Traversa, *Small*, 14 (2018) 1801231.
2. C. Bernuy-Lopez, L. Rioja-Monllor, T. Nakamura, S. Ricote, R. O'Hayre, K. Amezawa, M. Einarsrud and T. Grande, *Materials*, 11 (2018) 196.
3. Y.P. Xia, Z.Z. Jin, H.Q. Wang, Z. Gong, H.L. Lv, R.R. Peng, W. Liu and L. Bi, *J. Mater. Chem. A*, 7 (2019) 16136.
4. Y. Tian, Z. Lü, X. Guo and P. Wu, *Int. J. Electrochem. Sci*., 14 (2019) 1093.
5. X. Xu, L. Bi and X.S. Zhao, *J. Membrane Sci.*, 558 (2018) 17.
6. A.A. Solovyev, S.V. Rabotkin, A.V. Shipilova and I.V. Ionov, *Int. J. Electrochem. Sci*., 14 (2019) 575.
7. X. Xu, H.Q. Wang, J.M. Ma, W.Y. Liu, X.F. Wang, M. Fronzi and L. Bi, *J. Mater. Chem. A*, 7 (2019) 18792.
8. H. Jiang and F. Zhang, *Int. J. Electrochem. Sci*., 15 (2020) 959.
9. J.M. Ma, Z.T. Tao, H.N. Kou, M. Fronzi and L. Bi, *Ceram. Int.*, 46 (2020) 4000.
10. Y. N. Chen, T. Tian, Z. H. Wan, F. Wu, J. T. Tan and M. Pan, *Int. J. Electrochem. Sci.*, 13 (2018) 3827.
11. H.-S. Kim, H.B. Bae, W.C. Jung and S.-Y. Chung, *Nano. Lett.*, 18(2018) 1110.
12. G. L. Liu, W. Liu Q. Kou and S. J. Xiao, *Int. J. Electrochem. Sci*., 13 (2018) 2641.
13. L. dos Santos-Gómez, J. Zamudio-García, J.M. Porras-Vázquez, E.R. Losilla and D. Marrero-López, *J. Eur. Ceram. Soc.*, 40 (2020) 3080.
14. A. Arabaci, *Emerg. Mater. Res.*, 9 (2020) 296.
15. I. Shajahan, J. Ahn, P. Nair, S. Medisetti, S. Patil, V. Niveditha, G.U.B. Babu, H.P. Dasari and Jong-Ho Lee, *Mater. Chem. Phys.*, 216 (2018) 136.
16. Y. Itagaki, J. Cui, N. Ito, H. Aono and H. Yahiro, *J. Ceram. Soc. Jpn*, 126 (2018) 870-876.
17. Y. Jiang, H. Huang, M. Wang, W. Zhang and B. Wang, *J. Mater. Sci.*, 31 (2020) 6233.
18. Z. Huang, L. Fan, N. Hou, T. Gan, J. Gan, Y. Zhao and Y. Li, *J. Power Sources*, 451 (2020) 227809.
19. V. Vijaykumar, G. Nirala, D. Yadav, U. Kumar and S. Upadhyay, *Int. J. Energy Res.*, 44 (2020) 4652.
20. S. Soepriyanto, Y. Aristanti, T. Theresia, M. A. Sulthon, F. Baqir, W. P. Minwal and B. Dilasari, *J. Aust. Ceram. Soc.*, 55 (2019) 1161.
21. J. Cheng, C. Tian and J. Yang, *J. Mater. Sci.*, 30 (2019) 16613.
22. S.A. Kumar, P. Kuppusami, B. Vigneshwaran and Y.-P. Fu, *ACS Appl. Nano Mater.*, 2 (2019) 6300.
23. M. Anwar, S.A.M. Ali, A. Muchtar and M.R. Somalu, *J. Alloy. Compound.*, 775 (2019) 571.
24. S. Shawuti and M.A. Gulgun, *J. Power Sources*, 267 (2014) 128.
25. B. Zhu, S. Li and B.E. Mellander, *Electrochem. Commun.*, 10 (2008) 302.
26. M. Anwar, S.A.M. Ali, A. Muchtar and M.R. Somalu, *J. Alloy. Compound.*, 775 (2019) 571.
27. S. Shawuti and M.A. Gulgun, *J. Power Sources*, 267 (2014) 128.
28. B. Zhu, S. Li and B.E. Mellander, *Electrochem. Commun.*, 10 (2008) 302.

29. C. Slim, L. Baklouti, M. Cassir and A. Ringuedé, *Electrochim. Acta*, 123 (2014) 127.
30. Q. Yang, B. Meng, Z. Lin, X. Zhu, F. Yang, and S. Wu, *J. Am. Ceram. Soc.*, 100 (2017) 686.
31. S.A. Kumar, P. Kuppusami, B. Vigneshwaran and Y.-P. Fu, *ACS Appl. Nano Mater.*, 2 (2019) 6300.
32. K.A. Bhabu, J. Theerthagiri, J. Madhavan, T. Balu, G. Muralidharan and T. R. Rajasekaran, *J Mater. Sci.*, 27 (2016) 10980.
33. J. Ma, M. Zhang, L. Wang, X. Meng, W. Wang, J. Tang and G. Shao, *Int. J. Electrochem. Sci*., 16 (2021) 151054.
34. S. Taub, K. Neuhaus, H.-D. Wiemhöfer, N. Ni, J.A. Kilner and A. Atkinson, *Solid State Ionics*, 282 (2015) 54.
35. H. Wang, T. Hu and G. Xi, *Ceram. Int.*, 46 (2020) 8695.
36. W. Zhang, T. Hu, R. Shi and H. Wang, *Int. J. Electrochem. Sci*., 15 (2020) 304.